

A Comparative Study Between 3-Axis and 5-Axis Additively Manufactured Samples and their Ability to Resist Compressive Loading

N.Kaill*, R.I.Campbell*, P.Pradel*, G.A.Bingham⁺

*Loughborough Design School, Loughborough University, United Kingdom

⁺De Montfort University, United Kingdom

Abstract

One of the main limitations of parts made with Material Extrusion (ME) is their anisotropic mechanical behaviour. This behaviour limits the functionality of these components in multi-directional loading conditions. A critical factor for this mechanical behaviour is the poor bonding between layers. 5-axis ME has the capability to orientate the printed layers in order to limit the effect of poor inter-laminar bonding. Previous studies have investigated 5-axis ME, but not fully explored 5-axis capabilities of this manufacturing technique. To address this gap, this paper compares the mechanical behaviour of 3-axis and 5-axis ME samples when subjected to compressive loading. The results demonstrate how depositing material in “3D layers” can improve the consistency of a sample’s mechanical behaviour. This study indicates that 5-axis ME can enable more isotropic behaviour in printed samples.

Introduction

Material extrusion (ME) is the most prevalent category within additive manufacturing (AM) (1). ME is the process by which a material, in a liquid state, is metered through a nozzle or orifice (2). The extruded bead of material meets the build plate or previous layer and adheres to it. Typically, the extruder head is moved in the x-y axes via a gantry system that allows the creation of the layer detail. Once the layer is completed either the printed head is raised, or the build plate lowered by the layer thickness. This accumulation of multiple layers builds three-dimensional geometries. From a mechanical perspective, ME components present an anisotropic mechanical behaviour, because the inter layer bonding is much weaker than the intra layer one (3–8).

According to the 2017 Wohlers report, functional parts are the largest single application for AM produced components, with 33.8% of AM printed parts created for this purpose (9). For ME parts to be utilised for functional end-use applications, they must withstand complex multi-directional loadings. To address this limitation, the authors speculated that 5-axis ME could be utilised to improve parts’ mechanical behaviour by aligning the filament in the direction of the loads. In a previous paper, it was established that multi-axis ME can indeed improve the mechanical behaviour of ME parts (10). However, that study was limited to 4.5 axes due to one of the rotational axes being locked perpendicularly. This limitation was suitable for the geometrical complexity of the examined parts, but it did not address the difference in mechanical behaviour between fully 5-axis and 3-axis samples. Similarly, other studies that have looked into curved layer deposition have utilised a DELTA parallel robot (5,11) resulting in parts that were limited by the fixed position of the nozzle.

This paper will expand on previous work by exploiting 5-axis capabilities through a highly curved geometry represented by a simple thin-walled dome. Due to its topology, this

geometry is appropriate to explore how to optimise the mechanical performance of ME parts by exploiting 5 axes capabilities to selectively orient the deposition of filament.

The geometry that was selected for this study is a dome with a internal radius of 15mm and a wall thickness of 3mm. This geometry was selected as it is a simple shape that would allow for 5-axis ME to be explored with the revlevant directionality associated with this AM method. The thickness was selected based on the number of shell that could be used via a 5-axis method, with seven shells being decided upon. With the internal radius set at 15mm to keep samples in line samples produced in previous studies using similar methods (10). Traditional compression sample may be able to produce cleaner results, but the geometry may restrict the investigation into full 5-axis ME. This restriction could impede the comparrison between three and five axis ME.

Method

A finite element analysis (FEA) simulation was conducted to determine the direction of the stress vectors within the geometry of the dome when loaded in compression in the direction of its vertical axis (Figure 1). The simulation was carried out within Solidworks CAD software (12). A section of the dome's geometry was used in the simulation, with the boundary surfaces being constrained to allow sliding. A force was then applied to the top of the section, to induce the resultant stress vectors. The simulation indicates that the vertical direction is the dominant direction of the stress vectors. The horizontal stress component was indicated to be the next dominant component. In Figure 1, the colour of the vectors denotes the magnitude of the stress, in Solidworks red is used to indicate high values, while green indicates a lower value. When a compressive force of 1000N is applied, the vertical stress vectors have a maximum value of 12.34MPa with the horizontal having a maximum value of 3.84MPa.

This information was then used to create printing strategies for the 5-axis samples, as the direction of these stress vectors indicates the direction that material should be deposited in. The process of creating a 5-axis sample is shown in Figure 2 and expanded upon below. A sample data set will be created that includes a concentric infill pattern, to deposit material aligned with these stress vectors.

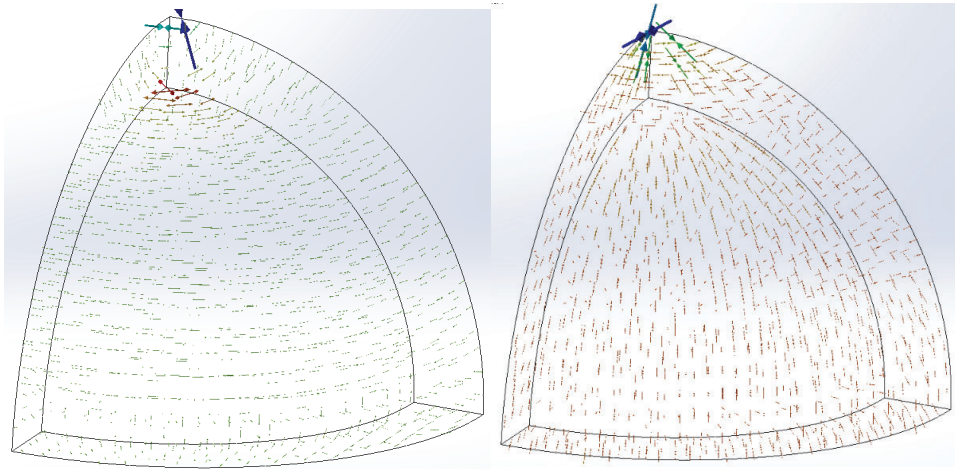


Figure 1: Simplified FEA of Model Section: (left) Horizontal Stress Vectors, (right) Vertical Stress Vectors

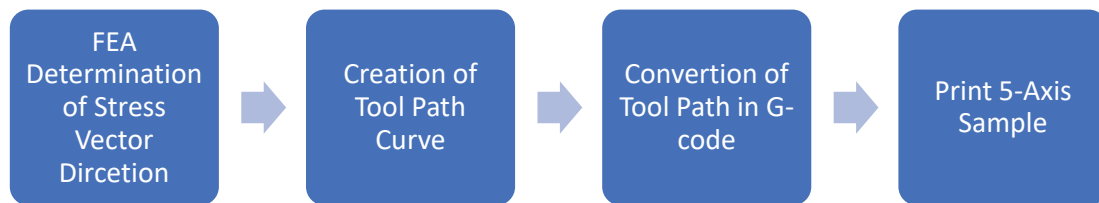
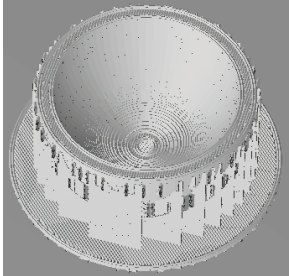
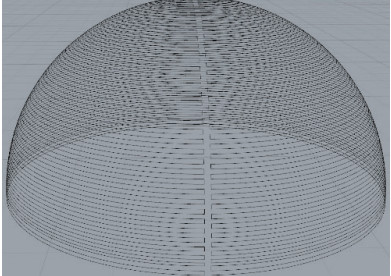
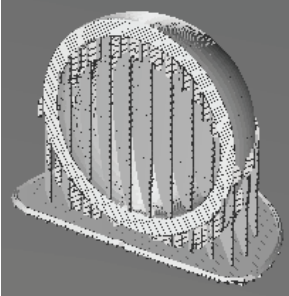
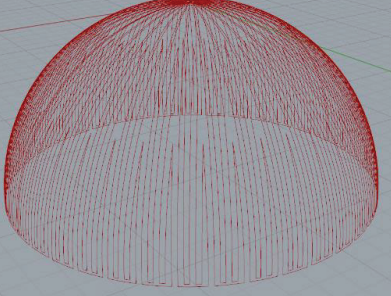
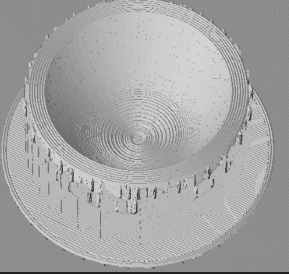
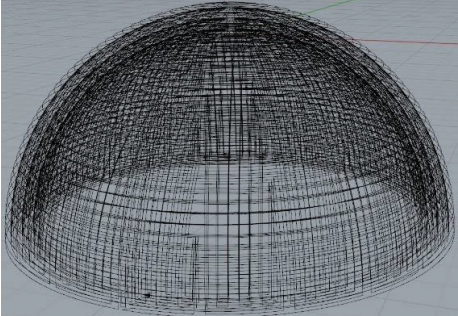


Figure 2: Flow Chart of 5-Axis Print Process

Once the direction of the stress vectors within the geometry has been understood, the print strategy can be created. As there is no “slicing” software available for converting CAD models to 5-axis tool paths, the tool paths for the experiment must be generated by the researchers. This process started with the print pattern created on a 2D plane, this pattern was then wrapped onto the surface that it will be printed on (i.e. the dome) and offset by half the thickness of the deposited material. Examples of the tool path for the initial layers of the samples are shown in Table 1. These curves are then scaled through parametric modelling techniques in Rhino Grasshopper (13), with each layer being joined to create a single continuous three-dimensional curve. This curve is then converted into a G-code for the 5-axis ME machine using proprietary software provided by the machine vendor (14).

Table 1: Sample Print Strategies

Print Strategy	3 Axis	5 Axis
Horizontal		
Vertical		
Concentric		
Combined		

The next stage was to create the printing jig as the base for the first layer to be deposited onto. Typical 3-axis ME processes require the use of support structures for printing 3D geometries (15). The printing jig acted as a support for the 5-axis machine and was reused across multiple prints. The 3-axis samples were printed utilising a MakerBot Replicator 2 Machine, whereas the 5-axis samples were printed utilising a 5axismaker machine. With the same material and deposition temperature being used on both machines to maintain consistency.

The initial set up period for the 5-axis machine required more time than a conventional 3-axis ME machine. This was due to the need to establish the central axis for each print, as it is entirely user-defined. To reduce the effect of this on the ability to print samples, the jig was

designed to be modular the purpose of this design choice was to allow the section of jig that the samples were printed on to be removed. This would ensure that the retained section of the print jig would be left in place maintaining the relative positioning in the machine. The process of depositing material in this fashion is shown in .

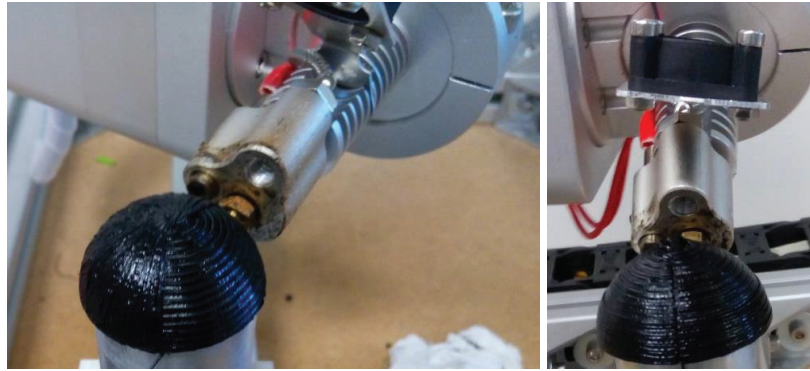


Figure 3: 5-Axis Material Extrusion: (left) Combined Print, (right) Horizontal Print

After printing each sample, its mass and dimensions were measured prior to the compression testing. The dimensions of the samples were measured through the use of a digital calliper, while the weight was measured through the use of digital scales. The average values are shown in Table 2. The printing times included show purely the printing time and do not include any post-processing the samples required. 5-axis samples required minimal post-processing due to the lack of support structures, whereas the 3-axis sample required significantly more time to remove the support structure. Examples of the 3-axis samples are shown in Figure 4. This figure illustrates the amount of support material that had to be removed prior to the compression testing.

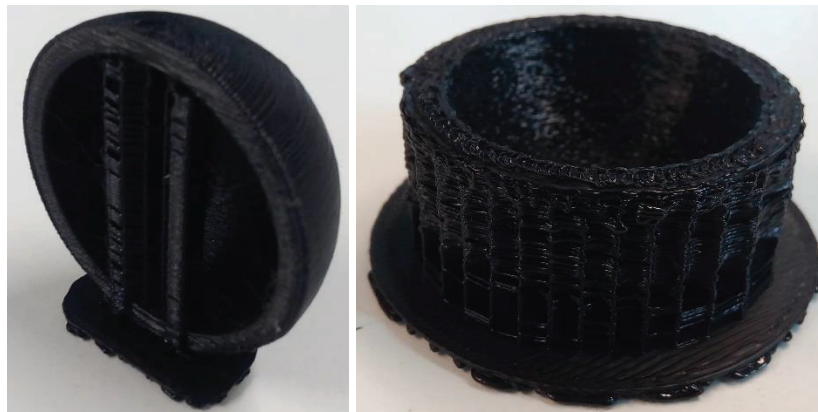


Figure 4: 3-Axis Material Extrusion with Support Structures: (left) Vertical Print, (right) Horizontal Print

Another interesting point that is highlighted in Table 22 is the difference in mass between the two printing processes, with all the 3-axis and 5-axis displaying similar mass within their own process. To establish fair comparison data sets, the CAD model used for the 3-axis sample was a solid dome with the average wall thickness of 5-axis samples. As the 3-axis samples display a thicker wall than the 5-axis samples, the residual support material may

be left attached to the surface of the samples. For each data set, 5 samples were produced in order to establish a reasonable average and to make identifying any outliers easier.

Table 2: Dome Study Average Measurements

Sample	Mean Diameter (mm)	Mean Thickness (mm)	Mean Mass (g)	Print Time (min)
3-Axis Horizontal	35.60	2.88	6.18	55
3-Axis Concentric	35.93	2.86	6.15	53
3-Axis Vertical	35.64	3.00	6.20	40
5-Axis Horizontal	35.78	2.74	5.22	94
5-Axis Vertical	35.86	2.85	5.38	73
5-Axis Combined	35.84	2.90	5.36	84

The axial compression testing was carried out on an Instron 3366 material test system with a 5kN load cell and a compression speed of 2mm.s^{-1} . The purpose of this test procedure was to establish the different mechanical behaviours of the test samples in regard to their respective stiffness, ductile behaviour and maximum compressive loading. The experimental setup is illustrated in Figure 5.

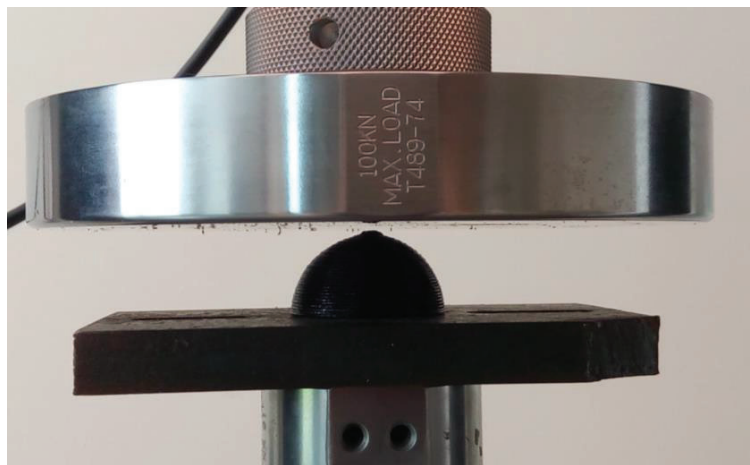


Figure 5: Compression Testing Set-up

Results and Discussion

The data from the compression testing of each sample were tabulated into an excel spreadsheet, for all 5 samples in each data set. The mean average for each set of samples is displayed in Figure 6.

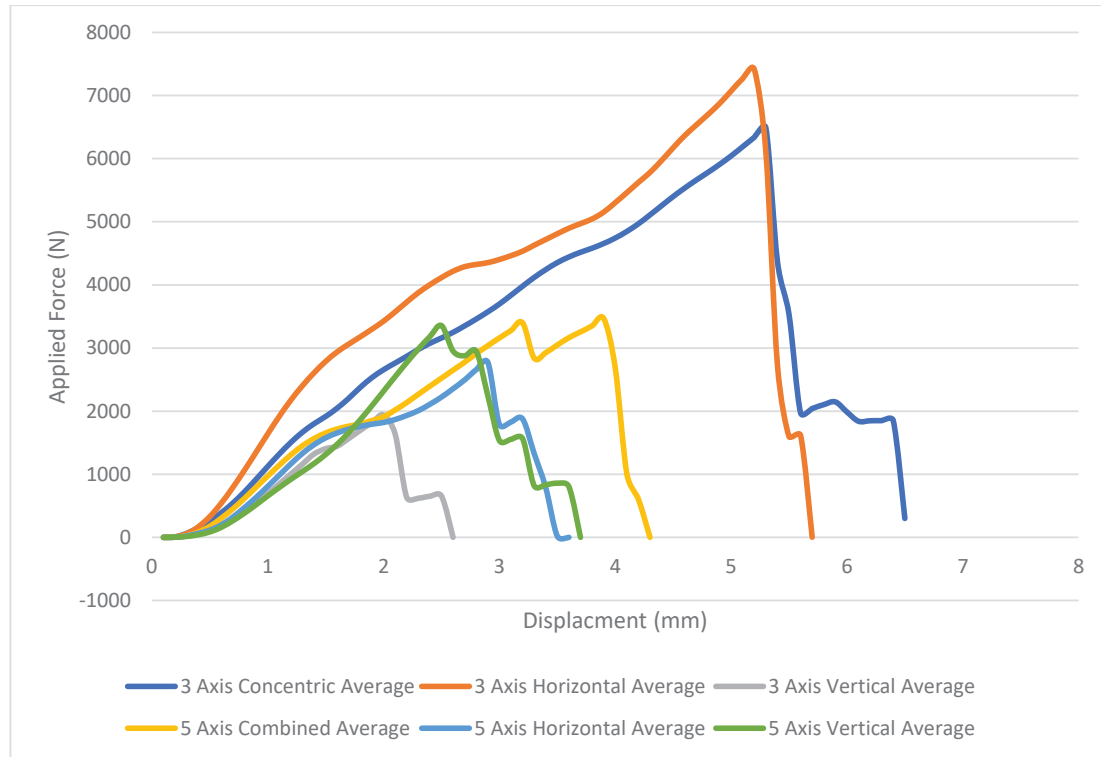


Figure 6: Average Compression Test Results for Dome Samples

The results of this study contain some unexpected findings. What stands out in Figure 6 is how the 3-axis Horizontal and Concentric samples were able to withstand significantly more load compared to all the other samples. Two possible explanations could be at play. First, the load was applied in one direction to a continuous symmetrical geometry enabling the stacked layers to be in constant compression. This led to the poor inter-laminar bonding not being a major limiting factor until the sample began to deform radially, at which point, the sample failed catastrophically. What is implicated here is that these samples were in compression until failure, meaning the samples behaved more like a strut than a thin-walled dome. This leads to the second explanation. All the samples followed similar failure behaviour, that of catastrophic failure. This differs from previous studies done by the Izmir Institute of Technology in Turkey that has analysed thin-walled domes (16). In that work, a dome deforms by first flattening its top, then the centre section is forced into space beneath the dome. Comparing the failure behaviours of the samples within this study the wall thickness is too high to allow for this plastic deformation. The sample shown within Figure 7 shows how much the 3-axis samples typically deformed prior to catastrophically failing. The specific sample shown is from a 3-axis horizontal sample. The top surface was deformed to the point where the centre should be forced through the centre; however, the thickness prevented this type of plastic deformation due to the amount of material present. The 3-axis vertical samples followed this

failure behaviour but at a significantly lower applied force, compared to all other samples. An explanation is that the forces were able to shear the interlaminar bonding, with minimal plastic deformation occurring. This confirms how significantly intralayer and interlayer bonding and thus print orientation affect the mechanical behaviour of 3-axis samples (16–19).

As to why the 3-axis Concentric and Horizontal samples displayed different values this can be explained by analysing their infill patterns. The concentric 3-axis samples had a concentric infill pattern while the horizontal pattern had a linear infill pattern. The linear nature of the infill pattern allowed it to resist some of the radial deformation allowing for the sample to withstand further loading. In comparison, the concentric infill pattern could only rely on inter-road bonding with each layer, to resist the radial deformation.

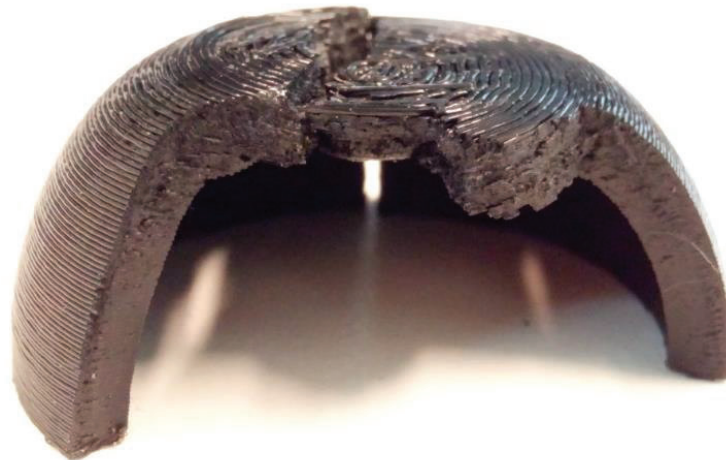


Figure 7: 3-Axis Horizontal Sample Post Compression Testing

To understand why our samples' failure behaviour differs from other work conducted on similar geometries, a sample 3-axis horizontal sample was printed with a wall thickness of 1.2mm, Figure 8 depicts the failure deformation of these samples. Notably, these samples follow the failure behaviour that was expected for this geometry, with initial plastic deformation occurring when a force of 500N was applied to the sample. The outcome of this clarification experiment indicates that there is a wall-thickness boundary condition for this type of geometry. This boundary condition drastically alters the failure behaviour of the samples and the amount of force they can withstand. This result highlights that if the desired geometries are not likely to allow plastic deformation and bending to occur, 5-axis ME may not be the most suitable manufacturing process. This would be an important factor where isotropic behaviour may not be required.

Another aspect of the 3-axis sample that may have impacted the results come from the support structures themselves. The support structures used in sample creation were break away supports made of the same PLA material as the sample. This means that the support material and any remaining support material could impact the compression test results. Particularly in regard to the different support structures used to create the 3-axis samples, and how this extra material can alter the compression behaviour of the samples.

Furthermore, this indicates that there is a further area of research indicated within this study, i.e. to look at samples with smaller wall thickness. A comparison could be made between how 3 and 5 axis samples differ in their compressive resistance when following this different failure behaviour.



Figure 8: Thin-Walled 3-Axis Horizontal Sample

The initial shape chosen for this study was selected based upon the assumption that they would follow the failure behaviour similar to those seen in other studies (20) while being a suitably complex shape that could be still be created via ME manufacturing techniques. A dome represented the simplest shape that incorporated one axis of rotational symmetry and can be printed with 2 axes of rotation. The method for creating the required tool path that enabled 5-axis deposition has highlighted that it is possible to create complex tool paths related to a known surface. This means that more complex geometries that would highlight the benefits of 5-axis could also be created and tested, in order to further explore the potential benefits of 5-axis ME. Focusing purely on the 5-axis samples, the vertical print strategy was able to withstand more applied force than the horizontal print strategy. This does indicate that orientating material to resist the 1st principle stress vector does improve the samples' mechanical behaviour. Moreover, the combined print strategy was able to resist more force over a prolonged period. This implies that alternating print patterns that resist a combination of the dominant principle stresses can create samples that display improved mechanical behaviour. This is a potential area of further research that would focus on how much material needs to be deposited along the different dominant stress vectors dependent on their magnitude. This is best explained in Figure 9, which contains a sample created to demonstrate how the alternating shells were deposited. More complicated shell patterns are possible in order to create samples that allow for bending moments to create plastic deformation in a non-catastrophic manner. This would allow for better control over failure behaviours and allow samples to behave in a more isotropic manner.

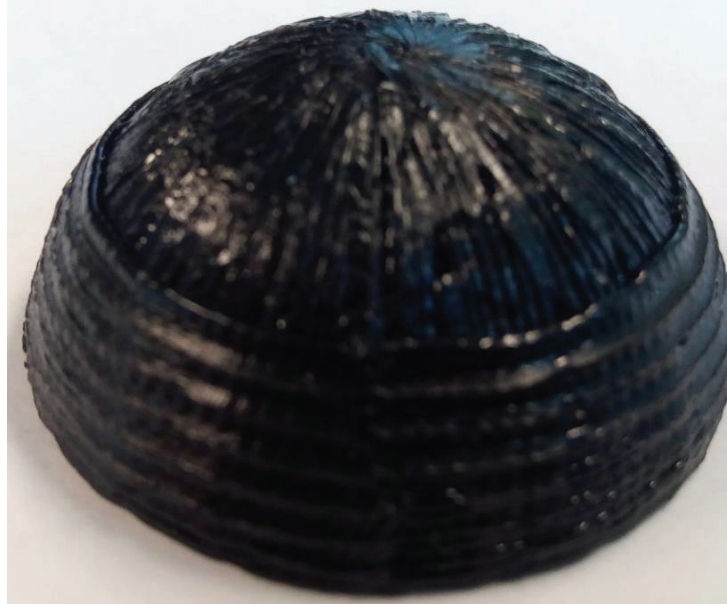


Figure 9: 5-Axis Combined Print Strategy Demo Sample

The 5-axis samples were not able to withstand as much compressive force as the 3-axis horizontal samples. This would indicate that only part of these samples acted in compression until failure. The rest of the sample would then be acting in tension, to create a bending moment in the sample as illustrated in Figure 10.

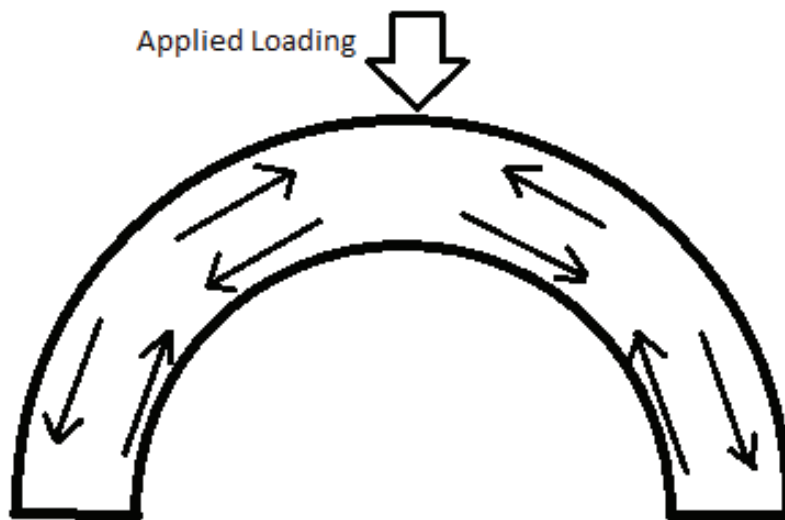


Figure 10: Illustration of Internal Compression/Tension Present in 5-Axis Samples

While this mechanical behaviour did not allow the 5-axis samples to withstand as much force as some of the 3-axis samples, it does indicate that these samples behave more isotopically, since all three build orientations had rather similar mechanical properties. This is an interesting result that could lead to further research and applications in industry.

Conclusion

Research into 5-axis ME is currently rather underdeveloped. As such, experimentation is required to improve the understanding of the limitations and benefits of this technology. The 3-axis ME results produced by this work did not generate the expected failure behaviour. However, the 5-axis samples did display the predicted mechanical behaviour in terms of which samples performed best in the compression loading test. This indicates that a combination print strategy has some potential to improve mechanical behaviour in ME samples, but that further research is required to explore its applicability. The anisotropy of most current ME process was shown most dramatically in the difference between the 3-axis vertical samples and the 3-axis horizontal samples. Orientating the print through 90° changed the load-bearing capability of samples by a factor of 3.5. Overall, 5-axis deposition along principle stress vector directions enabled the anisotropic nature of ME to be reduced. Such behaviour has the potential to expand the use of this manufacturing process for mechanical prototypes and end-use products.

A limitation of the 5-axis ME process that was used was that there is no automated software available to create the tool paths required for printing. Generating bespoke tool paths for samples could lead to further research in what is the best way to align material in a 5-axis context.

A future area of research will be to continue to explore 5-axis ME with the inclusion of reinforcing fibres that can be aligned in the direction of printing. At the time of writing this work is currently being carried out with a view to further publications.

References

1. Wohlers T, Gornet T. History of Additive Manufacturing. Wohlers Rep 2014 - 3D Print Addit Manuf State Ind. 2014;1–34.
2. Wohlers TT, Associates W. Wohlers Report 2012: Additive Manufacturing and 3D Printing State of the Industry Annual [Internet]. Wohlers Associates; 2012. Available from: <https://books.google.co.uk/books?id=ovVXNAEACAAJ>
3. Martínez J, Diéguez JL, Ares E, Pereira A, Hernández P, Pérez JA. Comparative between FEM models for FDM parts and their approach to a real mechanical behaviour. In: Procedia Engineering. Zaragoza; 2013. p. 878–84.
4. Dawoud M, Taha I, Ebeid SJ. Mechanical behaviour of ABS: An experimental study using FDM and injection moulding techniques. J Manuf Process [Internet]. 2016;21:39–45. Available from: <http://dx.doi.org/10.1016/j.jmapro.2015.11.002>
5. Singamneni S, Roychoudhury A, Diegel O, Huang B. Modeling and evaluation of curved layer fused deposition. J Mater Process Technol [Internet]. 2012;212(1):27–35. Available from: <http://dx.doi.org/10.1016/j.jmatprotec.2011.08.001>
6. Jami H, Masood SH, Song WQ. Dynamic response of FDM made ABS parts in different part orientations. Vol. 748, Advanced Materials Research. Seoul; 2013. p. 291–4.
7. Huang B, Singamneni SB. Curved Layer Adaptive Slicing (CLAS) for fused deposition modelling. Rapid Prototyp J. 2015 Jun;21(4):354–67.
8. Ahn S, Montero M, Odell D, Roundy S, Wright PK. Anisotropic material properties of fused deposition modeling ABS. Rapid Prototyp J. 2002 Oct;8(4):248–57.
9. Kianian B. Wohlers Report 2017: 3D Printing and Additive Manufacturing State of the Industry, Annual Worldwide Progress Report: Chapters titles: The Middle East, and

- other countries. 22nd ed. Wohlers Associates, Inc.; 2017.
10. Gardner JA, Kaill N, Campbell RI, Bingham GA, Engström DS, Balci NO. Aligning Material Extrusion Direction with Mechanical Stress via 5-Axis Tool Paths. 2018;2005–19.
 11. Diegel O, Singamneni S, Huang B, Gibson I. Getting Rid of the Wires: Curved Layer Fused Deposition Modeling in Conductive Polymer Additive Manufacturing. *Key Eng Mater*. 2011;467–469:662–7.
 12. Solidworks CAD Software [Internet]. DASSAULT Systems. Available from: <https://www.solidworks.com/>
 13. Rutten D. Grasshopper 3D (Version 0.9.0076) [Windows]. Roger de Flor, Barcelona, Spain: Robert McNeel and Associates; 2009.
 14. 5 Axisworks. No Title [Internet]. 2018. 2018 [cited 2018 Jul 31]. Available from: <http://www.machsupport.com/software/mach3/>
 15. Lee J-Y, An J, Chua CK. Fundamentals and applications of 3D printing for novel materials. *Appl Mater Today* [Internet]. 2017;7:120–33. Available from: <http://linkinghub.elsevier.com/retrieve/pii/S2352940717300173>
 16. Tanikella NG, Wittbrodt B, Pearce JM. Tensile strength of commercial polymer materials for fused filament fabrication 3D printing. *Addit Manuf* [Internet]. 2017;15:40–7. Available from: <http://dx.doi.org/10.1016/j.addma.2017.03.005>
 17. Davis CS, Hillgartner KE, Han SH, Seppala JE. Mechanical strength of welding zones produced by polymer extrusion additive manufacturing. *Addit Manuf* [Internet]. 2017;16:162–6. Available from: <http://dx.doi.org/10.1016/j.addma.2017.06.006>
 18. Leutenecker-Twelsiek B, Klahn C, Meboldt M. Considering Part Orientation in Design for Additive Manufacturing. In: *Procedia CIRP*. 2016.
 19. McLouth TD, Severino J V, Adams PM, Patel DN, Zaldivar RJ. The Impact of Print Orientation and Raster Pattern on Fracture Toughness in Additively Manufactured {ABS}. *Addit Manuf* [Internet]. 2017;18. Available from: <http://www.sciencedirect.com/science/article/pii/S2214860417301781>
 20. Tasdemirci A, Sahin S, Kara A, Turan K. Crushing and energy absorption characteristics of combined geometry shells at quasi-static and dynamic strain rates: Experimental and numerical study. *Thin-Walled Struct* [Internet]. 2015;86:83–93. Available from: <http://dx.doi.org/10.1016/j.tws.2014.09.020>